noaffinity chromatography was with an affinity-purified anti-Hh-N polyclonal antibody (*11*). Whole-cell protein extracts were prepared by solubilization in radioimmunoprecipitation assay buffer [1% NP-40, 0.5% sodium deoxycholate, 0.1% SDS, 50 mM tris-HCl (pH 7.5), 150 mM NaCl, 1 mM EDTA, and a protease inhibitor cocktail of phenylmethylsulfonyl fluoride, leupeptin, aprotinin, pepstatin, and E64]. *Drosophila* larval extracts were prepared by dounce homogenization of dissected, inverted larvae in RIPA. All incubations and centrifugations were at 0° to 4°C.

34. J. Taipale *et al.*, *Nature* **406**, 1005 (2000).
35. Masses of HhNp and HhNp^{C85S} were determined by MALDI-TOF mass spectrometry on a Voyager DE STR Biospectrometry Workstation (PerSeptive Biosystems) in linear mode. Affinity-purified protein samples were desalted and concentrated using C4 ZipTips (Millipore), with binding taking place in the presence of 10% acetonitrile. Eluted samples and standards were mixed 1:1 with 10 mg/ml sinapinic acid (Sigma) in 50% acetonitrile/0.3% (v/v) trifluoroacetic acid and spotted. Horse skeletal myoglobin {[M+H]1+ (avg.) = 16952.56; Sigma} and bovine trypsinogen (23981.89; Sigma) were included in samples for internal mass calibration.
36. C. H. Chen *et al.*, *Cell* **98**, 305 (1999).
37. HhNp-containing protein samples were prepared for C4 reversed-phase chromatography by acetone precipitation (six to eight volumes, –20°C), resuspension in hexafluoroisopropanol (neat; with brief water-bath sonication) and solubilization with 70% formic acid (2 volumes); samples were immediately injected. Gradient fractionations were performed at 60°C with acetonitrile and *n*-propanol (1:1) as organic modifiers and 0.15% (w/v) TFA in mobile phases; 1-min fractions were collected during a 1% gradient developed from 40 to 54% (total organic). HhNp-containing fractions were lyophilized and analyzed on Western blots. Film densities of early- and late-eluting peaks were determined and summed for ratio analysis.
38. Supported by the Swiss National Science Foundation and the Howard Hughes Medical Institute. We thank E. Frei for the genomic *Drosophila* library, A. McMahon for the mouse Shh cDNA, and A. Erkner for generating UAS-Shh transformants.

16 July 2001; accepted 24 July 2001
Published online 2 August 2001;
10.1126/science.1064437
Include this information when citing this paper.

Requirement of Tissue-Selective TBP-Associated Factor $TAF_{II}105$ in Ovarian Development

Richard N. Freiman,[1] Shane R. Albright,[1,2] Shuang Zheng,[1,2] William C. Sha,[1] Robert E. Hammer,[2,3] Robert Tjian[1,2]*

Transcription factor TFIID, composed of TBP and TAF_{II} subunits, is a central component of the RNA polymerase II machinery. Here, we report that the tissue-selective $TAF_{II}105$ subunit of TFIID is essential for proper development and function of the mouse ovary. Female mice lacking $TAF_{II}105$ are viable but infertile because of a defect in folliculogenesis correlating with restricted expression of $TAF_{II}105$ in the granulosa cells of the ovarian follicle. Gene expression profiling has uncovered a defective inhibin-activin signaling pathway in $TAF_{II}105$-deficient ovaries. Together, these studies suggest that $TAF_{II}105$ mediates the transcription of a subset of genes required for proper folliculogenesis in the ovary and establishes $TAF_{II}105$ as a cell type–specific component of the mammalian transcriptional machinery.

The control of transcription in a spatial and temporal fashion is essential for the proper development and differentiation of specialized cell types that define multicellular organisms. The intricate regulation of transcription relies on the coordinate assembly of large multiprotein complexes at promoter and enhancer regions of specific genes. The transcription factor TFIID is responsible for core promoter recognition and for directing RNA polymerase II to select genes in response to upstream activators (*1*, *2*). Although TFIID was initially thought to be ubiquitous in expression and universal in function, the discovery of putative tissue-restricted components of TFIID prompted us to reevaluate the gene-specific function of this transcription complex. The first cell type–specific subunit of TFIID, called $TAF_{II}105$, was identified as a polypeptide that coprecipitated with TATA-binding protein (TBP) and the other TAF_{II}s from a highly differentiated human B cell line but not other cell lines (*3*). The primary amino acid sequence of $TAF_{II}105$ revealed that it is related to the more broadly expressed human $TAF_{II}130$ (*4*, *5*) and its *Drosophila* homolog $dTAF_{II}110$ (*6*). The recent identification of yeast $TAF_{II}48$ has revealed a weak similarity to the COOH-terminal third of $TAF_{II}105$; however, the NH_2-terminal coactivator domain is absent in $TAF_{II}48$, suggesting that the metazoan subunits function in regulating programs of gene expression specific to multicellular organisms (*7*). Indeed, the circumstances of $TAF_{II}105$'s discovery suggest that it might be involved in regulating B cell–specific gene expression. Recent experiments demonstrating that human $TAF_{II}105$ can interact with nuclear factor kappa B and OCA-B (also called OBF-1) support this hypothesis (*8*, *9*). To examine further whether $TAF_{II}105$ indeed functions in a tissue- and gene-specific manner in mammals, we set out to characterize the biological role of $TAF_{II}105$ in the mouse.

[1]Department of Molecular and Cell Biology, [2]Howard Hughes Medical Institute, University of California at Berkeley, Berkeley, CA 94720–3204, USA. [3]Department of Biochemistry and the Green Center for Reproductive Biology Sciences, University of Texas Southwestern Medical Center at Dallas, Dallas, TX 75390, USA.

*To whom correspondence should be addressed. E-mail: jmlim@uclink4.berkeley.edu

To determine the tissue-selective nature of $TAF_{II}105$ expression in mice, we measured the relative levels of $TAF_{II}105$ and $TAF_{II}130$ mRNA in selected tissues. Ribonuclease (RNase) protection assays (Fig. 1A) revealed high levels of $TAF_{II}130$ in all tissues examined, except for the liver. In contrast, $TAF_{II}105$ transcripts were expressed most highly in the testes and ovary, whereas lower levels were detected in most other tissues. On the basis of restricted expression of $TAF_{II}105$ mRNA largely in the gonads, we turned to identifying tissue-selective functions of $TAF_{II}105$.

First, we confirmed that $TAF_{II}105$ is a component of mouse TFIID in ovaries (Fig. 1B). Total cell extracts prepared from mouse ovaries were precipitated with monoclonal antibodies to TBP (anti-TBP); the presence of $TAF_{II}250$, $TAF_{II}105$, and TBP was confirmed by Western blot analysis (Fig. 1B, lane 2) (*10*). No TFIID subunits were detected in the control precipitation with a nonspecific antibody (lane 1). These data establish that $TAF_{II}105$ is a bona fide TFIID component in murine ovaries.

Given the highly restricted pattern of $TAF_{II}105$ expression in mice, it seemed plausible that disruption of the endogenous $TAF_{II}105$ gene by homologous recombination would not compromise viability. A $TAF_{II}105$ genomic targeting vector (Fig. 2A) was constructed carrying the neomycin (NEO) resistance gene inserted in reverse orientation to the 3′ end of the $TAF_{II}105$ gene (*11*). This construct was transfected into mouse embryonic stem (ES) cells, generating several clones containing one copy of the wild-type (WT) gene and one copy of the mutant $TAF_{II}105$ gene (Fig. 2B). Heterozygous ES cells were injected into mouse blastocysts, and chimeric mice were established that transmitted a mutant copy of the $TAF_{II}105$ gene through the germ line. A polymerase chain reaction (PCR)–based genotyping assay (Fig. 2C) was performed on the progeny of heterozygous matings to identify homozygous knockout (KO) animals. Western blot analysis of B cell extracts derived from mice of each genotype (Fig. 2D)

confirmed that $TAF_{II}105$ protein expression was abrogated (*10*). The $TAF_{II}105$-specific band was detected only in cells derived from WT and HET mice and was absent in the KO mice. These data demonstrate that we successfully disrupted both copies of the endogenous $TAF_{II}105$ gene and produced mice lacking $TAF_{II}105$ protein.

Thus far, heterozygous matings have yielded 242 progeny, with $TAF_{II}105$ genotypes of 63 WT, 119 HET, and 60 KO. This distribution approximates the expected Mendelian ratio of 1:2:1 from heterozygous crosses and indicates that the lack of $TAF_{II}105$ has no deleterious effect on viability. Because $TAF_{II}105$ was originally identified in human B cells, several parameters of immune function were examined and shown to be unaffected by the deletion of $TAF_{II}105$ (*12*). Thus, $TAF_{II}105$ may play a redundant role in the immune system with another factor, such as $TAF_{II}130$, that can compensate for the absence of $TAF_{II}105$ in our KO mice.

Female homozygous KO mice exhibited a striking abnormality in fertility. In all the natural matings of hybrid $TAF_{II}105$ KO female mice, no progeny were obtained. In contrast, male homozygous $TAF_{II}105$ KOs were fertile. The infertility of hybrid homozygous KO females was consistent through six generations, suggesting that the defect is due to disruption of the $TAF_{II}105$ gene and not some spurious mutation. To elucidate the basis of this infertility, we assessed whether null females cycled, exhibited behavioral estrous, and mated. All eight of the –/– females that were test-mated, bred, as evidenced by the presence of a copulatory plug. This observation suggested that the defect in $TAF_{II}105$-null females may be ovarian and/or uterine. To distinguish between these possibilities, we induced pseudopregnancy in null females and performed embryo transfers (*13*). Four out of the five null females that carried transferred eggs became pregnant, gave birth to viable litters, lactated, and displayed normal maternal behavior. This finding suggested that the defect in fertility was not uterine but ovarian in origin.

To define the ovarian defect, we assessed whether null females ovulated naturally or were responsive to hormonal treatment to induce ovulation. Four nonhormone-treated –/– females that bred with stud males ovulated (~seven eggs per female); however, none of the 26 eggs collected developed in culture. To assess whether null females could be induced to ovulate, we hormonally primed age-matched 8-week-old +/– and –/– females. Whereas eight treated +/–females ovulated 120 eggs, only a single egg was recovered from the null females. The failure to retrieve more than a single egg from treated null females could be a consequence of a defect in oocyte development and/or maturation. To distinguish between these possibilities, we isolated and weighed the ovaries from hormonally primed females and assessed ovarian histology. The ovaries from null females were half the weight (4.3 mg ± 1.3 mg; n = 8 mice) of the ovaries from age-matched fertile +/– females [8.9 mg ± 2.2 mg; n = 8 mice (*14*)]. Histologically, ovaries from treated null females had very few maturing follicles and only an occasional antral follicle (Fig. 3A). In contrast, ovaries from +/+ and +/– females displayed follicles at all developmental stages. Whereas 2-month-old null females failed to undergo induced ovulation, 5- to 6-month-old females did respond, albeit poorly, to hormone treatment. From 13 treated older null females mated to stud males, 36 eggs were collected, none of which cleaved in culture. This suggests a defect in oocyte maturation and/or fertilization. These data are consistent with the complete lack of fertility seen in $TAF_{II}105$ KO females at all reproductive ages.

To further confirm the relevance of the apparent lack of maturing follicles in hormone-primed females to the observed infertility, we localized the site of $TAF_{II}105$ expression in the ovary. RNA in situ hybridization analysis revealed that $TAF_{II}105$ is expressed exclusively in the granulosa cells surrounding the developing oocyte (Fig. 3B). In contrast, $TAF_{II}130$ is expressed throughout the ovary, including the oocyte, granulosa cells, and corpus luteal cells. Whereas $TAF_{II}130$ expression is readily detected in the $TAF_{II}105$ KO ovary, there is a lack of $TAF_{II}105$ expression in the mutant ovaries. There is a concomitant lack of maturing follicles in the KO ovary. Thus, the in situ data, together with the histologic observations, indicate that $TAF_{II}105$ is likely critical for the timely development and/or proliferation of the

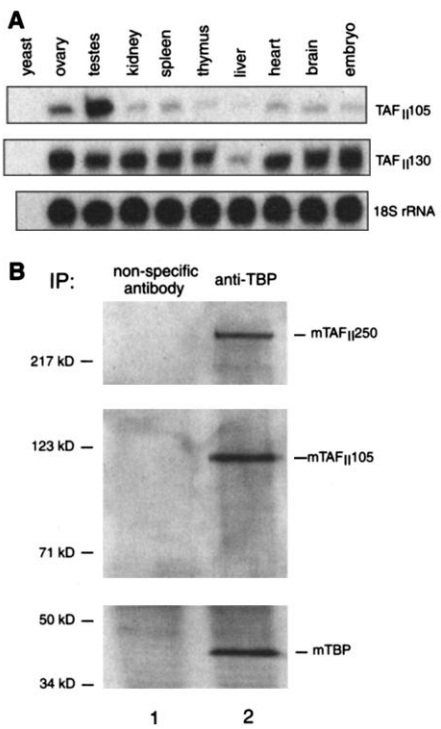

Fig. 1. $TAF_{II}105$ is differentially expressed in mouse tissues. (**A**) $TAF_{II}105$ is highly expressed in the testes and ovary. RNase protections were carried out as described (*25*). Protected products specific for $TAF_{II}105$, $TAF_{II}130$, and an 18S rRNA control are indicated on the right. Mouse tissues from which total RNAs were derived are shown. A yeast total RNA sample was included in each experiment as a negative control. (**B**) Mouse $TAF_{II}105$ specifically coprecipitates with TFIID in extracts derived from mouse ovaries. Immunoprecipitation (IP) of ovarian extracts with a nonspecific antibody (lane 1) or anti-TBP (lane 2) followed by Western analysis with anti-$TAF_{II}250$, anti-$TAF_{II}105$, and anti-TBP is shown. Molecular mass markers are indicated on the left; mouse $TAF_{II}250$-, $TAF_{II}105$-, and TBP-specific bands are indicated on the right.

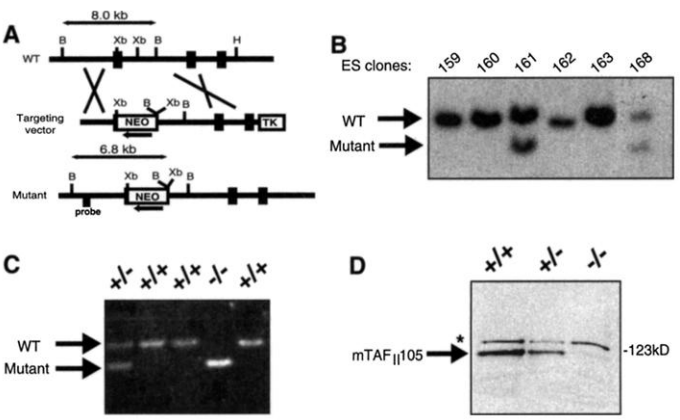

Fig. 2. Generation of a $TAF_{II}105$ KO mouse. (**A**) The strategy used to disrupt the endogenous $TAF_{II}105$ gene. Double arrows of 8.0 and 6.8 kb represent the WT and mutant alleles of $TAF_{II}105$, respectively. Restriction sites of the genomic locus are indicated (B, Bam HI; Xb, Xba I; and H, Hind III), and a small black box indicates the probe used for Southern blot analysis. (**B**) Southern blot analysis of several ES clones containing both WT and mutant copies of the $TAF_{II}105$ locus. (**C**) PCR-based genotyping of DNA derived from the progeny of $TAF_{II}105$ heterozygous crosses. (**D**) Mouse $TAF_{II}105$ protein is absent in cells derived from homozygous $TAF_{II}105$ knockout mice. Western blot analysis of LPS-stimulated splenic B cell extracts with anti-$TAF_{II}105$ is shown. Genotypes of protein sources are shown. The mouse $TAF_{II}105$-specific protein band is indicated, and a nonspecific cross-reacting protein band is marked with an asterisk.

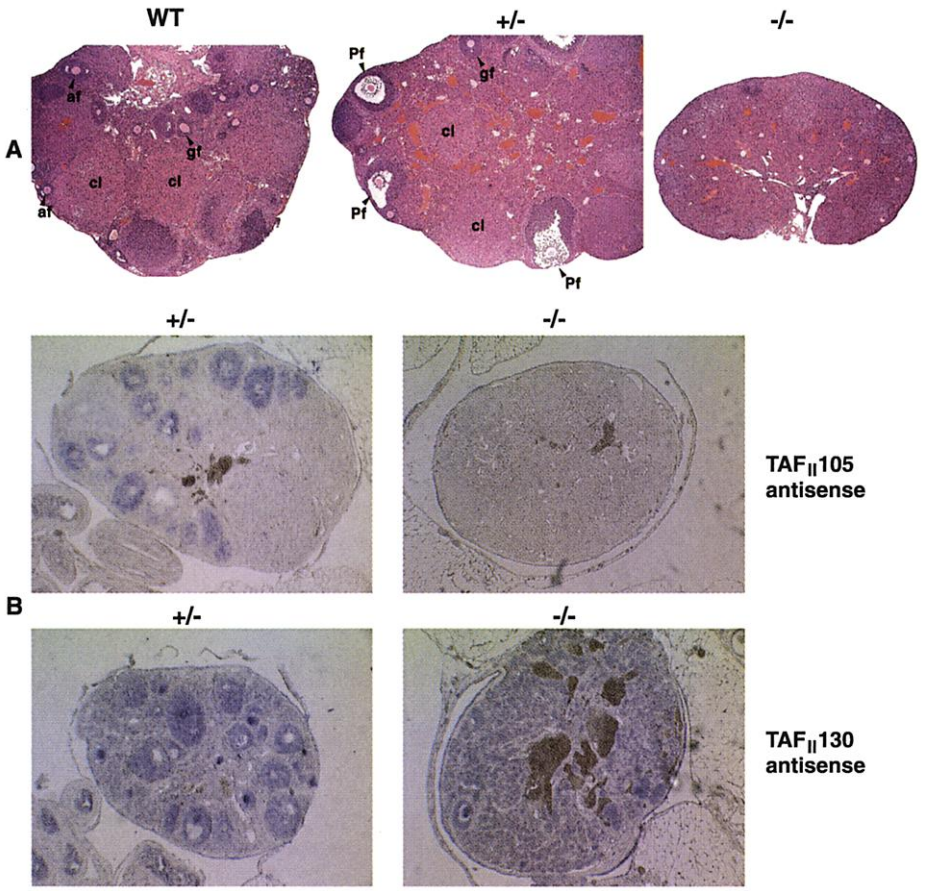

Fig. 3. Expression of TAF$_{II}$105 mRNA is restricted to the granulosa cells of the ovarian follicle. (**A**) TAF$_{II}$105-deficient ovaries are smaller than WT ovaries and lack mature follicles. Hematoxylin-and eosin-stained ovary sections are shown (*26*). Genotypes of ovaries are indicated, and ovarian follicles are labeled as preovulatory follicle (Pf), antral follicle (af), growing follicle (gf), and corpus luteum (cl). (**B**) In situ hybridization with TAF$_{II}$105- and TAF$_{II}$130-specific antisense RNA probes (*26*). Genotypes of ovary sections and corresponding probes are shown.

	Microarray	RNase protection	+/-	-/-
Inhibin βB subunit	8.2	12.8		
Aromatase p450	7.2	11.7		
Inhibin βA subunit	5.8	13.6		
Cyclin D2	5.4	2.8		
17-β–hydroxysteroid dehydrogenase type 1	5.2	7.9		
Follistatin	4.8	10.7		
Inhibin α subunit	3.0	3.1		
β-actin	1.1	1.3		

Fig. 4. Ovarian-specific genes down-regulated in TAF$_{II}$105-deficient ovaries. Total RNA was isolated from dissected ovaries, and 7 μg was used to synthesize cRNA probes for hybridization to murine 11K microarrays (Affymetrix). Gene expression changes of over 11,000 genes were compared between the +/– and –/– ovaries, and genes that decreased by twofold or greater in the –/– ovaries were identified by genechip software (Affymetrix). Fold reductions in the TAF$_{II}$105-deficient ovaries of a subset of these genes involved in female reproduction are listed. RNase protection assays (*25*) and corresponding genotypes of the RNA source are shown.

granulosa cells of the ovarian follicle required for proper ovarian function.

To understand the molecular mechanism underlying the folliculogenesis defect caused by TAF$_{II}$105 deletion, we set out to identify gene expression pathways that might be disrupted in our TAF$_{II}$105-deficient ovaries. Oligonucleotide-based microarrays containing over 11,000 murine genes were probed with RNA derived from HET and KO ovaries dissected from 8-week-old age-matched and hormonally synchronized females. Only 132 genes (1%) of the genes assayed were down-regulated twofold or more (*14*). A number of genes known to function in folliculogenesis and known to be important for female fertility (*15*) were down-regulated (3- to 14-fold) in the TAF$_{II}$105-deficient ovaries (Fig. 4). Most notably, the expression of multiple components of the inhibin-activin-follistatin pathway was severely compromised in the TAF$_{II}$105 KO ovaries. Inhibins and activins are transforming growth factor–β (TGF-β) family members that modulate the release of follicle-stimulating hormone from the pituitary and regulate estrogen synthesis within the ovary (*16*). In addition, the expression of aromatase p450, a critical enzyme responsible for the conversion of androgens to estrogens in granulosa cells, decreased dramatically. Finally, cyclin D2, which is essential for granulosa cell proliferation and female fertility (*17*) was also down-regulated in the mutant ovaries. Consistent with the role of this specific set of genes, down-regulating their expression correlates with the improper regulation of folliculogenesis seen in the TAF$_{II}$105-deficient ovaries and may explain the infertility observed in these mice.

These studies establish that there are cell type–specific components of TFIID in mammals and that specialized transcription initiation complexes function in regulating tissue-specific programs of gene expression. Such cell type–specific general factors function analogously to sigma factors of the prokaryotic transcription system, which regulate promoter selectivity of RNA polymerase (*18*). These findings complement the recent findings of Fuller and colleagues, who have shown that a testes-specific homolog of *Drosophila* TAF$_{II}$80 called Cannonball is required for germ cell development in male flies (*19*). In addition, the TBP-homolog TRF2 has been shown to be required for embryogenesis in *Caenorhabditis elegans* and *Xenopus*, but it is required only for spermiogenesis in the mouse (*20–24*). Taken together, these studies emphasize the critical roles of the general transcriptional machinery in regulating cell type– and gene-specific transcription in metazoans.

The restricted expression of TAF$_{II}$105 in the granulosa cells of fertile ovaries strongly correlates with the apparent defective function of this cell type in TAF$_{II}$105 KO mice. In addition, we have identified a number of putative target genes, specifically down-regulated in the TAF$_{II}$105-deficient ovaries, that are known to play a critical role in folliculogenesis (*15*). On the basis of TAF$_{II}$105 expression in the granulosa cells of the ovary and TAF$_{II}$105 being associated with TBP in ovary extracts, we envision that TAF$_{II}$105 mediates the transcription of a subset of granulosa cell-specific genes, some of which have been identified in our microarray experiments (*14*). Future biochemical studies will examine whether TAF$_{II}$105 directly mediates the expression of these target genes. It is tempting to speculate that TAF$_{II}$105 is also involved in regulating ovarian gene expression in humans. Therefore, characterizing how TAF$_{II}$105 functions in the mouse may help reveal the molecular basis of certain types of female infertility in humans.

References and Notes

1. J. A. Goodrich, T. Hoey, C. J. Thut, A. Admon, R. Tjian, *Cell* **75**, 519 (1993).
2. C. P. Verrijzer, K. Yokomori, J. L. Chen, R. Tjian, *Science* **264**, 933 (1994).
3. R. Dikstein, S. Zhou, R. Tjian, *Cell* **87**, 137 (1996).
4. N. Tanese, D. Saluja, M. F. Vassallo, J. L. Chen, A. Admon, *Proc. Natl. Acad. Sci. U.S.A* **93**, 13611 (1996).
5. G. Mengus, M. May, L. Carré, P. Chambon, I. Davidson, *Genes Dev.* **11**, 1381 (1997).
6. T. Hoey *et al.*, *Cell* **72**, 247 (1993).
7. S. L. Sanders, P. A. Weil, *J. Biol. Chem.* **275**, 13895 (2000).
8. A. Yamit-Hezi, R. Dikstein, *EMBO J.* **17**, 5161 (1998).
9. O. Wolstein, A. Silkov, M. Revach, R. Dikstein, *J. Biol. Chem.* **275**, 16459 (2000).
10. Total protein extracts were prepared from mouse ovaries of 8-week-old mice that were hormonally synchronized for 48 hours by injection of 7 IU of PMS-G. Ovaries were harvested, washed in phosphate-buffered saline, dounced in extraction buffer [200 mM KCl, 100 mM tris (pH 7.9), 0.2 mM EDTA, 10% glycerol, and 0.1% NP-40], and incubated for 1 hour on ice. Either 20 μl of anti-Myc negative control or 20 μl of anti-TBP/protein A–Sepharose CL-4B (Amersham Pharmacia) beads were incubated with 0.3 ml of ovary extract for 4 hours at 4°C. Immune complexes were washed twice in 0.2 M KCL, twice in 0.5 M KCl, and then twice in 0.2 M KCl on ice. Beads were boiled in sample buffer and separated on either a 7.5 or 10% SDS–polyacrylamide gel electrophoresis (SDS-PAGE) gel. Western blot analysis was carried out with rabbit polyclonal antisera diluted to 1:5000 for anti-$TAF_{II}105$ or to 1:2500 for anti-$TAF_{II}250$ and TBP. The secondary antibody to immunoglobulin G–horseradish peroxidase (Pierce, Rockford, IL) was diluted to 1:5000, and proteins were visualized with enhanced chemiluminesence (Amersham Pharmacia). For the protein samples in Fig. 2D, splenocytes derived from mice of each genotype were activated with lipopolysaccharide (LPS), lysed in sample buffer, and separated by a 6% SDS-PAGE gel.
11. Overlapping phage clones containing a portion of the $TAF_{II}105$ gene were isolated from a mouse 129Sv genomic library and subcloned to generate pBT3. Not I–linearized pBT3 was electroporated into R1 ES cells. The targeting event removed half of exon h located in the 3′ end of the $TAF_{II}105$ gene, replacing it with a *neo* cassette in the reverse orientation. Genomic DNA was isolated from neomycin-resistant ES clones, digested with Bam HI, and analyzed by Southern blot analysis against a ^{32}P-labeled genomic fragment. Targeting efficiency was about 1.6%. Heterozygous ES cells were injected into blastocysts to establish founder chimeric mice, and chimeric mice that transmitted to the germ line were bred to homozygosity. To genotype mice, tail genomic DNA was analyzed in a single PCR reaction containing three primers (105G2, AACATGTAATGGATTTTCT; 105G4, GGTCTGTATTTCCTTAATGG; and Neo2, CTAATTCATCAGAAGCTGAC), which amplifies a 200–base pair (bp) fragment and a 150-bp fragment from the wild-type and mutant $TAF_{II}105$ alleles, respectively. Western blot analysis was used to confirm the loss of full-length $TAF_{II}105$ and the absence of COOH-terminally truncated forms of $TAF_{II}105$. Heterozygous $TAF_{II}105$ mice were back-crossed to the inbred C57BL/6J strain (Jackson Laboratories, West Grove, PA).
12. R. N. Freiman, R. Tjian, unpublished data.
13. R. L. Brinster, H. Y. Chen, M. E. Trumbauer, M. K. Yagle, R. D. Palmiter, *Proc. Natl. Acad. Sci. U.S.A.* **82**, 4438 (1985). $TAF_{II}105^{-/-}$ females were bred with vasectomized males, and the presence of a copulatory plug indicated a successful mating. On day 0.5 postcoitum, WT B6SJL F_2 hybrid two-cell eggs were transferred into one oviduct of each −/− pseudopregnant female as previously described. Superovulation was induced by a standard hormone regimen, and ovulated eggs were collected 13 hours after injection of human chorionic gonadotropin as previously described.
14. Supplementary Web material is available on *Science* Online at www.sciencemag.org/cgi/content/full/293/5537/2084/DC1.
15. J. A. Elvin, M. M. Matzuk, *Rev. Reprod.* **3**, 183 (1998).
16. P. G. Knight, *Front. Neuroendocrinol.* **17**, 476 (1996).
17. P. Sicinski *et al.*, *Nature* **384**, 470 (1996).
18. C. A. Gross *et al.*, *Cold Spring Harbor Symp. Quant. Biol.* **63**, 141 (1998).
19. M. A. Hiller, T.-Y. Lin, C. Wood, M. T. Fuller, *Genes Dev.* **15**, 1021 (2001).
20. L. Kaltenbach, M. A. Horner, J. H. Rothman, S. E. Mango, *Mol. Cell* **6**, 705 (2000).
21. J. C. Dantonel, S. Quintin, L. Lakatos, M. Labouesse, L. Tora, *Mol. Cell* **6**, 715 (2000).
22. G. J. Veenstra, D. L. Weeks, A. P. Wolffe, *Science* **290**, 2312 (2000).
23. I. Martianov *et al.*, *Mol. Cell* **7**, 509 (2001).
24. D. Zhang, T. L. Penttila, P. L. Morris, M. Teichmann, R. G. Roeder, *Science* **292**, 1153 (2001).
25. Antisense riboprobes labeled with ^{32}P–uridine 5′-triphosphate were synthesized with Maxiscript (Ambion, Austin, TX). Plasmid pAA12 was linearized with Acc65I and transcribed with T7 RNA polymerase to synthesize an antisense $TAF_{II}105$ probe; plasmid pZ33 was linearized with Pst I and transcribed with T3 RNA polymerase to synthesize an antisense $TAF_{II}130$ probe. Hybridizations were carried out with RPA III (Ambion). To detect $TAF_{II}105$ and $TAF_{II}130$ levels, we used 30 μg of total RNA (Ambion), and to detect 18S rRNA levels, we used 1 μg of total RNA. For assays in Fig. 4, 3 μg of total RNA derived from +/– and –/– ovaries was used.
26. Ovaries from 6-week-old females were removed from hormonally primed mice, dissected, weighed, and fixed in 10% neutral buffered formalin. Specimens were embedded in paraffin, sectioned at 5 μm, stained with hematoxylin and eosin, and examined and photographed at the identical magnification with a Leica DMR microscope equipped with a MetaMorph Imaging System. For in situ hybridizations, ovaries were dissected from HET and KO females and fixed in a 6:3:1 cocktail of ethanol, formaldehyde (37%), and acetic acid overnight at 4°C. Ovaries were dehydrated in an ethanol series and Histoclear (National Diagnostics, Atlanta, GA) and then embedded in paraffin. Sections of 14 μm were prepared and probed with digoxygenin (DIG)–labeled antisense RNA probes (Roche). An alkaline phosphatase-conjugated antibody to DIG (Roche) was used at a 1:2000 dilution to detect specific RNAs with the substrates NBT and BCIP (Gibco-BRL), and RNAs were visualized by the formation of a blue/purple precipitate.

27. We thank M. Haggart for technical assistance; L. Chu for contributions to this project; D. Bhattacharya and L. Liang for advice with the immunology assays; O. Kelly, B. Martin, and M. Dionne for instruction with in situ hybridizations; N. Hernandez for providing the anti-TBP; A. Ladurner for providing control and $TAF_{II}250$ antibodies; R. Henry for advice with immunoprecipitations; D. Schichnes and S. Ruzin of the CNR biological imaging facility; A. Winoto for RI ES cells; K. Thomas for a 129Sv genomic library; W. Skarnes for mouse blastocyst injections; R. Harland, A. Hochheimer, M. Holmes, C. Inouye, Y. Isogai, B. Lemon, and M. Levine for comments; and J. Lim for preparation of the manuscript. R.N.F. is a fellow of the Leukemia and Lymphoma Society. Supported in part by a grant from NIH to R.T.

24 April 2001; accepted 16 July 2001

A Gene Expression Map for *Caenorhabditis elegans*

Stuart K. Kim,[1]* Jim Lund,[1] Moni Kiraly,[1] Kyle Duke,[1] Min Jiang,[1] Joshua M. Stuart,[2] Andreas Eizinger,[1] Brian N. Wylie,[3] George S. Davidson[3]

We have assembled data from *Caenorhabditis elegans* DNA microarray experiments involving many growth conditions, developmental stages, and varieties of mutants. Co-regulated genes were grouped together and visualized in a three-dimensional expression map that displays correlations of gene expression profiles as distances in two dimensions and gene density in the third dimension. The gene expression map can be used as a gene discovery tool to identify genes that are co-regulated with known sets of genes (such as heat shock, growth control genes, germ line genes, and so forth) or to uncover previously unknown genetic functions (such as genomic instability in males and sperm caused by specific transposons).

The completion of the *C. elegans* genome sequence has identified nearly all of the genes in the genome (19,282 genes) (*1*), but the function for most of these genes remains mysterious. A scant 6% of them have been studied with the use of classical genetic or biochemical approaches (1135 genes), and only about 53% show homology to genes in other organisms (10,303 genes) (*2*). The current challenge is to develop high-throughput functional genomics procedures to study many genes in parallel in order to elucidate gene function on a global scale (*3–8*). In one approach, a compendium of gene expression profiles was assembled from a large number of yeast DNA microarray experiments (*9*), which made it possible to ascribe potential functions to previously unknown genes by comparing their expression results to those of genes with known functions. Here, we have established a compendium of gene expression profiles for an animal, *C. elegans*.

We combined data from many DNA mi-

[1]Department of Developmental Biology and Genetics, Stanford University Medical School, Stanford, CA 94305, USA. [2]Stanford Medical Informatics, 251 Campus Drive, MSOB X-215, Stanford, CA 94305, USA. [3]Computation, Computers and Mathematics Center, Sandia National Laboratories, Albuquerque, NM 87185–0318, USA.

*To whom correspondence should be addressed. E-mail: kim@cmgm.stanford.edu